Experimental Analysis of High-Resolution Soft X-ray Microscopy

Weilun Chao[1 2 **], Erik H. Anderson[1], Gregory Denbeaux[1], Bruce Harteneck[1], Angelic L. Pearson[1], Deirdre Olynick[1], Gerd Schneider[1], David Attwood[1 2]

[1] Center for X-ray Optics, Lawrence Berkeley National Laboratory, CA 94720
[2] University of California at Berkeley, CA 94720

ABSTRACT

The soft x-ray, full-field microscope XM-1 at Lawrence Berkeley National Laboratory's (LBNL) Advanced Light Source has already demonstrated its capability to resolve 25-nm features. This was accomplished using a micro zone plate (MZP) with an outer zone width of 25 nm. Limited by the aspect ratio of the resist used in the fabrication, the gold-plating thickness of that zone plate is around 40 nm. However, some applications, in particular, biological imaging, prefer improved efficiency, which can be achieved by high-aspect-ratio zone plates. We accomplish this by using a bilayer-resist process in the zone plate fabrication. As our first attempt, a 40-nm-outer-zone-width MZP with a nickel-plating thickness of 150 nm (aspect ratio of 4:1) was successfully fabricated. Relative to the 25-nm MZP, this zone plate is ten times more efficient. Using this high-efficiency MZP, a line test pattern with half period of 30 nm is resolved by the microscope at photon energy of 500 eV. Furthermore, with a new multilayer mirror, the XM-1 can now perform imaging up to 1.8 keV. An image of a line test pattern with half period of 40 nm has a measured modulation of 90%. The image was taken at 1.77 keV with the high-efficiency MZP with an outer zone width of 35 nm and a nickel-plating thickness of 180 nm (aspect ratio of 5:1). XM-1 provides a gateway to high-resolution imaging at high energy. To measure frequency response of the XM-1, a partially annealed gold "island" pattern was chosen as a test object. After comparison with the SEM image of the pattern, the microscope has the measured cutoff of 19 nm, close to the theoretical one of 17 nm. The normalized frequency response, which is the ratio of the power density of the soft x-ray image to that of the SEM image, is shown in this paper.

Keywords: soft x-ray microscope, XM-1, high aspect ratio, zone plate, resolution, gold island pattern.

1. INTRODUCTION

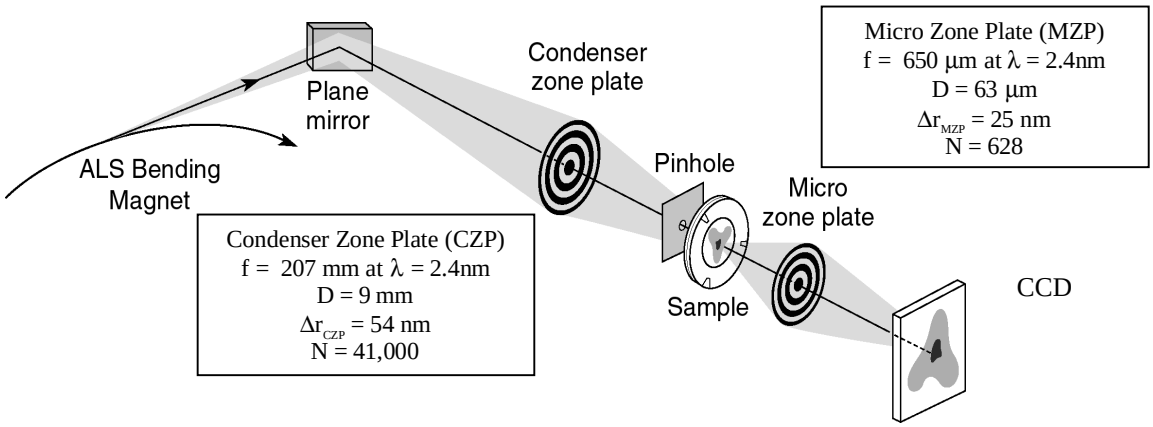

Figure 1. The layout of the soft x-ray microscope XM-1 at beamline 6.1.2 of the Advanced Light Source (ALS). Bending magnet radiation from the ALS is used to illuminate the sample, which is in air. The combination of numerical apertures of the two zone plates produces partially coherent imaging condition, with σ equal to $\Delta r_{MZP} / \Delta r_{CZP} = 0.45$

* Correspondence: wlchao@lbl.gov ; Phone: 510-486-4079; Fax: 510-486-4550; Lawrence Berkeley National Laboratory, 1 Cyclotron Road, MS 2-400, Berkeley, CA 94720.

The soft x-ray microscope XM-1 at LBNL's Advanced Light Source (ALS) synchrotron radiation facility is an extension of a visible light microscope to the soft x-ray region [1 2]. It uses radiation from a bending magnet in the ALS to illuminate its sample, which is in air. Because XM-1 is operated in the soft x-ray region (from 300 eV to 1.8 keV), it can be used to image wet samples up to 10 μm thick in the full-field transmission mode, which is an advantage over other high-resolution microscopes like TEM.

Figure 1 shows the layout of XM-1. Bending magnet radiation from the ALS is reflected by a plane mirror onto a condenser zone plate (CZP), which in turn focuses the radiation on the sample through a pinhole. The radiation passing through the sample is then imaged onto a charge-coupled device (CCD) using a micro zone plate (MZP). Both the CZP and MZP are fabricated in the Nanofabrication Laboratory in the Center for X-ray Optics (CXRO) [3]. The spatial resolution of the microscope is determined in part by the outer zone width of the MZP. Currently, the highest-resolution MZPs have an outer zone width of 25 nm (figure 2). With this zone plate, XM-1 has demonstrated its capability to resolve 25-nm-half-period features [4].

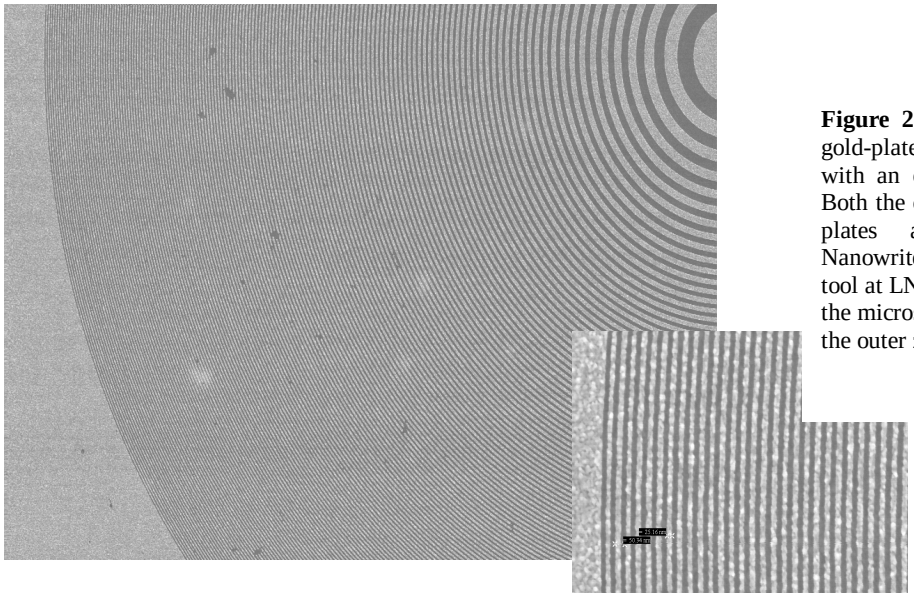

Figure 2. A SEM micrograph of the gold-plated micro zone plate (MZP) with an outer zone width of 25 nm. Both the condenser and the micro zone plates are fabricated with the Nanowriter electron beam lithography tool at LNBL. The spatial resolution of the microscope is determined in part by the outer zone width of the MZP.

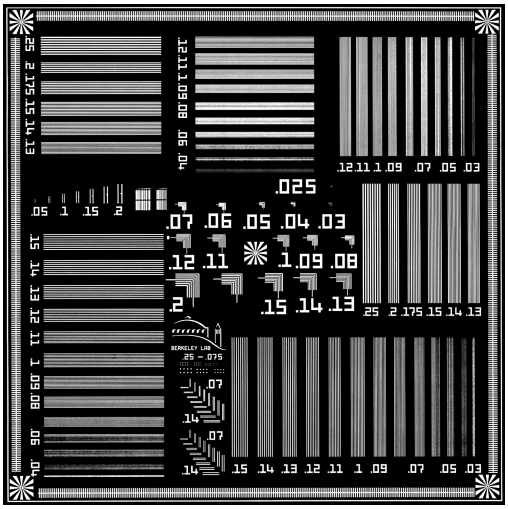

Figure 3. One of the test objects used for resolution measurement. This 120 μm X 120 μm test pattern plated with 40-nm-thick gold contains two sets of line patterns with linewidths from 30 nm to 250 nm. One set has line-to-space ratio of 1:1, the other has a ratio of 1:2. The center of the object has a set of elbow patterns with linewidths as narrow as 25 nm. This object is used in most of the measurements in this paper.

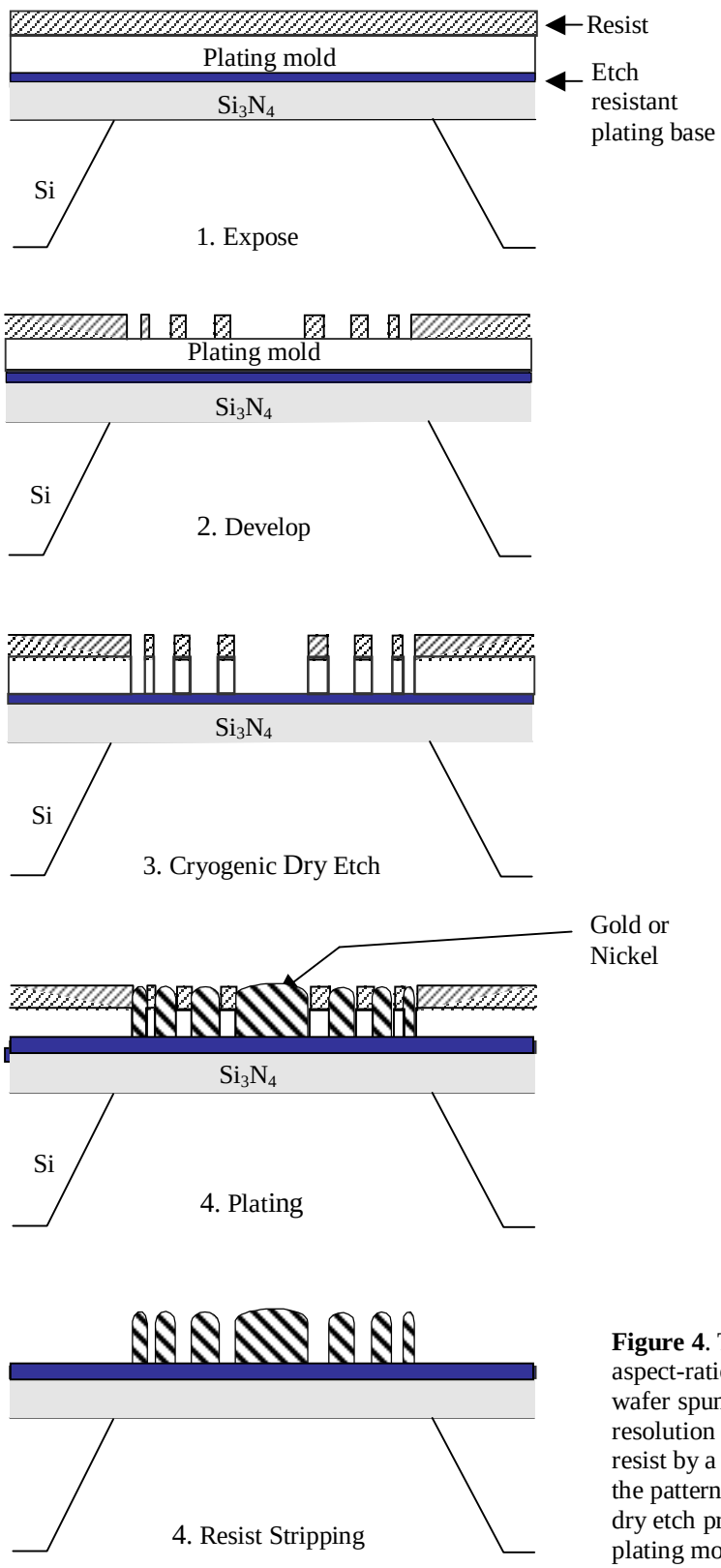

In addition to very high spatial resolution, the microscope also has a good energy spectral resolution, which is determined by the geometry of the CZP and the pinhole. The current spectral resolution $\lambda/\Delta\lambda$ with a stationary condenser illumination is around 700 over a 9-μm^2 field [5], which allows users to perform elemental-sensitive imaging including magnetic material imaging [6].

To characterize the spatial resolution of XM-1, several test objects with line patterns of different periods and duty cycles were fabricated using the same lithography tool as used for the zone plates. One of them, which is used in most of the measurements in this paper, is shown in figure 3. It was fabricated using the Nanowriter electron beam tool to write the pattern into Calixarene resist, followed by gold plating. The plating thickness of is nominally 40 nm.

2. HIGH-EFFICIENCY MICRO ZONE PLATE

The 25-nm-outer-zone-width MZP provides very high resolution. However, due to the current limitations in fabricating such a fine structure, the gold-plated MZP is relatively thin (about 40 nm). For some of our applications (in particular, biological imaging), where radiation dose is required to be minimal, improved efficiency of the MZP is preferred. This requires a high-aspect-ratio MZP. We accomplish this by the development of a bilayer-resist process.

In the bilayer-resist process, a high-resolution-resist layer and a layer of plating mold, a material that forms a mold for plating, are used for pattern formation (figure 4). The resist acts as a recording layer, where the pattern is written using a high-resolution electron beam. The

Figure 4. The bilayer-resist process is used to fabricate high-aspect-ratio zone plates. First, a Si-supported membrane wafer spun with a layer of plating mold and a layer of high-resolution resist is prepared. A pattern is then written into the resist by a high-resolution electron beam. After development, the pattern is transferred to the plating mold using a cryogenic dry etch process. The wafer is then plated. The resist and the plating mold are then stripped to obtain the final patterned object,

pattern is then transferred into the plating mold using a cryogenic dry etch process. This etch process is chosen because the use of the cold temperature (cryogenic) and gaseous etch chemicals (dry etching) reduces the vertical-sidewall etching. The patterned wafer is then plated with gold or nickel.

The bilayer-resist process allows fabrication of fine structures with relative high aspect ratio. In our case, HydrogenSilsesQuioxane (HSQ) and hardbaked AZPN114 are used as the resist and plating mold, respectively. The HSQ layer is about 40 nm thick and the structure is plated with either gold or nickel after the dry etching of the plating mold.

In our first attempt we began by fabricating 40-nm-outer-zone-width MZPs for better yield. The nickel-plating thickness of the zone plate is around 150 nm (aspect ratio of 4:1). Using one of these MZPs, the line patterns in the test object in figure 3 were imaged at the wavelength of 2.4 nm. The images of patterns with half periods of 30 nm and 40 nm and their corresponding lineouts are shown in figure 5. Both the 30-nm and 40-nm patterns are resolved by the microscope, with a corresponding modulation of 28% and 43%. Relative to the 25-nm-outer-zone-width MZP, this zone plate is 10 times more efficient.

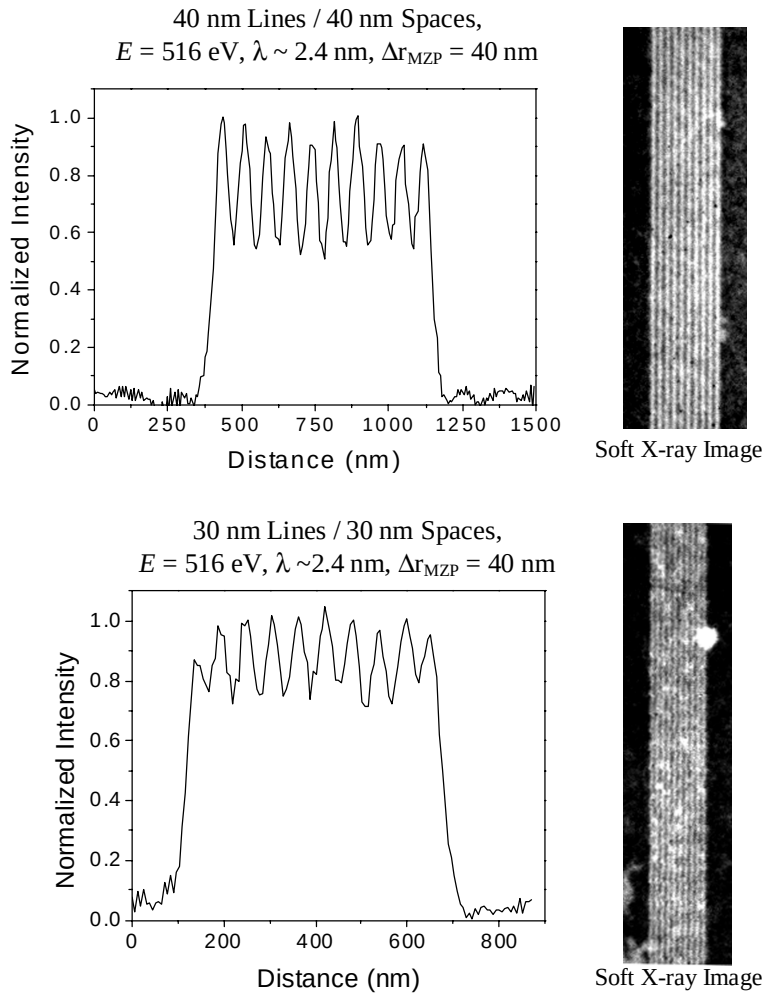

Figure 5. The line patterns with half periods of 30 nm and 40 nm were imaged with the 150-nm-thick, high-efficiency nickel MZP with the smallest zone width of 40 nm. Both 30-nm and 40-nm patterns are clearly resolved by the microscope, with the modulation of 28% in the 30-nm case.

Recently, 35-nm-outer-zone-width MZPs with a nickel-plating thickness of 180 nm (aspect ratio of 5:1) have been fabricated. They have been used in high-energy imaging experiments discussed in the following section.

3. HIGH-ENERGY IMAGING

As shown in figure 1, a plane mirror reflects bending magnet radiation to the microscope. The purpose of this mirror is to cut off high-energy photons. The nickel mirror used previously had a reflectivity of less than 15% for photon energies higher than the Ni L_3 edge, near 850 eV [7]. Motivated by interconnect [8] and magnetic material imaging (e.g., Ni and Gd), we upgraded the nickel mirror to a multilayer mirror [9]. This enables XM-1 to perform imaging with energies up to 1.8 keV. Figure 6 shows the accumulation of 5 images of a line pattern with a half period of 40 nm. It was taken with a 35-nm-outer-zone-width MZP with a thickness of 180 nm (aspect ratio of 5:1) at 1.77 keV ($\lambda \sim 0.7$ nm).

At this photon energy, the 40-nm-thick gold plating of the line pattern absorbs only about 10 % of the incoming light, as compared to 60% at the photon energy of 500 eV. Based on the relationship between a pattern's natural contrast (C) and the number of photons needed to be collected in the pattern's image (N) to obtain a given signal-to-noise ratio (SNR), i.e. $N \propto 1/C^2$, an image at the energy of 1.8 keV would require 61 times more photons than that imaged at 500 eV to acquire the same SNR. Furthermore, for a given number of incoming photons, the CCD camera converts 1.8 keV/500 eV ~ 4 times more electron-hole pairs at the energy of 1.8 keV than at 500 eV (for simplicity, the photon-energy dependence of the quantum efficiency is ignored) Thus, to have the same image fidelity, an image taken at 1.8-keV energy needs about 240 times more counts than that at 500-eV energy. All of our images taken at different photon energies have similar number of counts. Therefore, the SNR of an accumulation of 5 images at 1.77-keV energy is 240/5 ~ 50 times worse than that of a single image taken at 500-eV energy. This difference is shown clearly when the images in figure 5 and 6 are compared with each other.

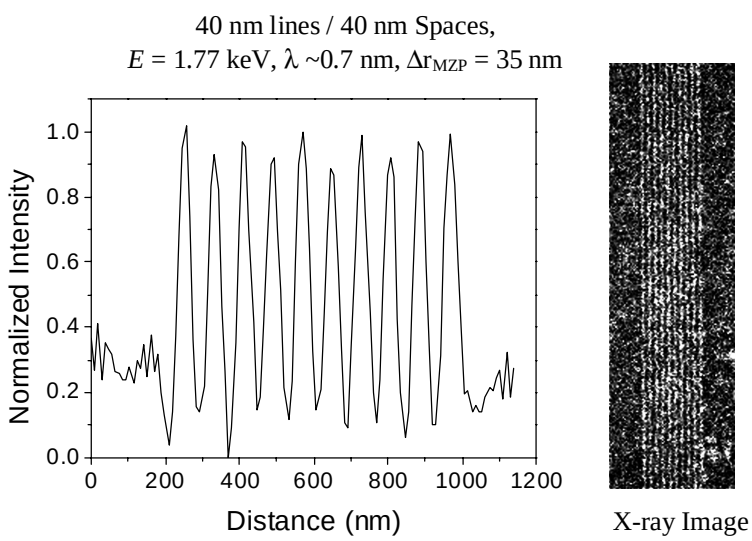

Figure 6. Shown are the accumulation of 5 images (after contrast and brightness adjustment) and the corresponding lineout of a line pattern with a half period of 40 nm taken at the energy of 1.77 keV. The MZP used in the imaging has the outer zone width of 35 nm and a nickel-plating thickness of 180 nm. The lineout shows a large modulation (90%) after averaging over the entire length of the image and normalized.

To obtain a low-noise lineout, the accumulated image is averaged along its length. Because of low absorption of the gold plating, the line-pattern's contrast in the CCD image is low. Normalization is needed to make the lineout more discernible. The normalized lineout is plotted in figure 6 and shows a surprisingly good modulation of 90%. Because the data analysis is sensitive to the high background and noise statistics, a further investigation of the modulation is in progress.

4. GOLD "ISLAND" SPECTRAL ANALYSIS

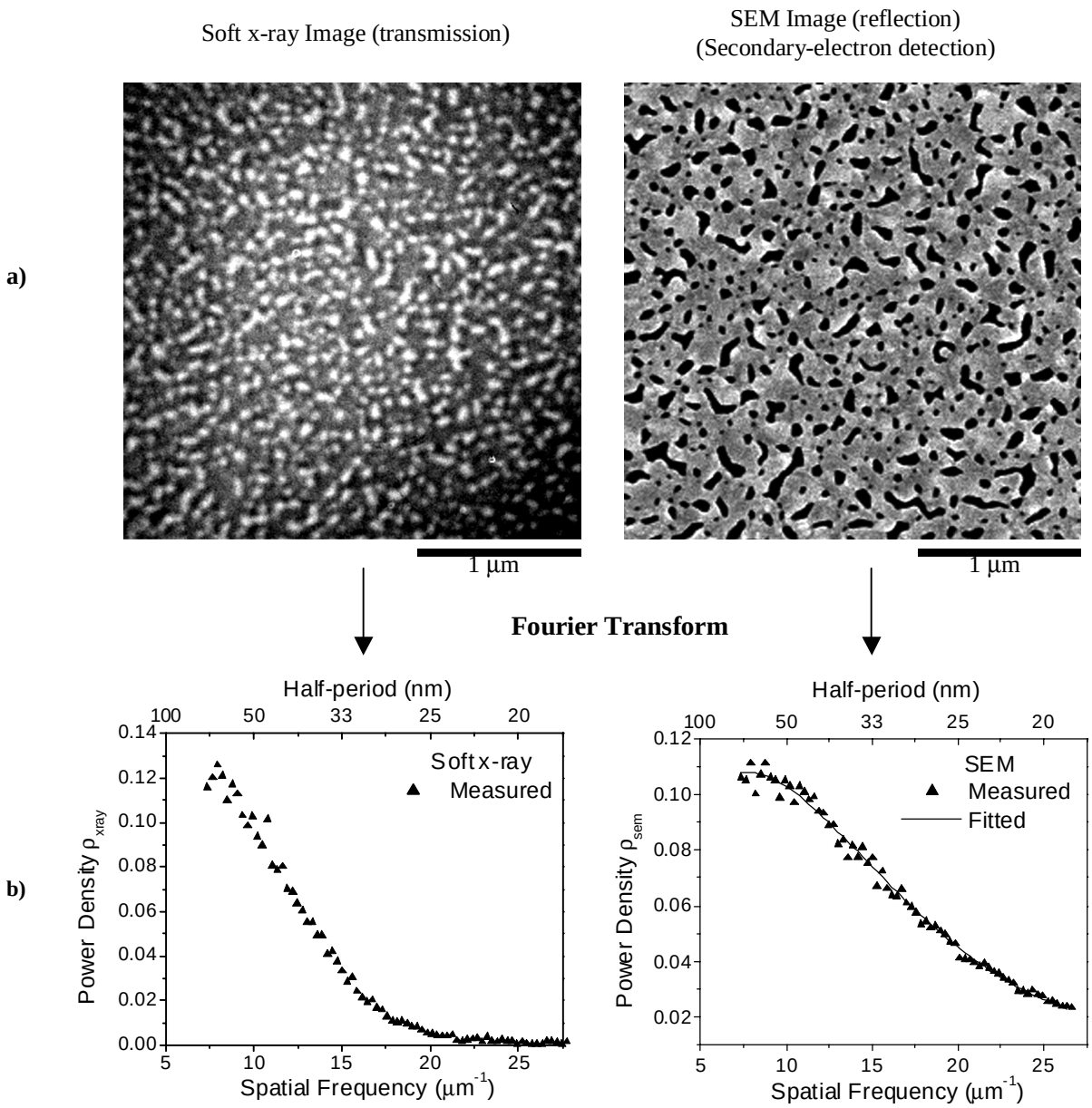

Figure 7. The gold "island" pattern was chosen for measurement of the frequency response of XM-1. a) The soft x-ray and SEM images of the gold pattern. The images were not taken at the same location. The pixel size for both images is 8 nm and the x-ray image was obtained with the 25-nm MZP at the wavelength of 2.4 nm. b) The power densities of the corresponding images. The density of the SEM image is fitted with polynomials to eliminate fluctuations in the data.

One of the deficiencies of the line patterns is that the response of the microscope is measured only at a single spatial frequency. Many patterns with different periods are required to obtain the response over a wide range of frequency. Moreover, when the period is small, it is difficult to obtain a high-quality pattern. The imperfections in the pattern will complicate the analysis of the images.

To overcome these difficulties, we employed a pattern of gold "islands" with sizes randomly distributed. This sample is prepared by annealing a 10-nm-thick gold layer on a thin Si_3N_4 membrane for an hour at 170 ^{0}C. At this temperature, the gold will tend to aggregate and form "islands". Because a large and pseudo-continuous range of feature sizes (from a few nm to about 100 nm) is obtained without any complicated nanofabrication processes, this pattern is ideal for measurement of frequency response of the microscope.

Figure 7a shows the soft x-ray image and SEM micrograph of the gold island pattern. The x-ray image was taken at a wavelength of 2.4 nm with the 25-nm-outer-zone-width lens described in figure 2. The projected pixel sizes are 8 nm for both images. The images were taken at different locations. However, this does not affect our analysis, as the dimensional distribution of the islands is the same at different locations due to the randomness of the gold islands. To obtain the power spectrum of the images, the images are first Fourier transformed, then averaged along the circumferences of circles centered at the zero frequency component (figure 7b). The power spectrum of the SEM image is fitted with polynomials to eliminate fluctuations in the spectrum.

Assuming the power spectrum of the SEM image to be the true spectrum of the pattern, a normalized frequency response of XM-1 is obtained by dividing the power spectrum of the soft x-ray image by that of the SEM image (figure 8). The normalized response shows that XM-1 has a 10% response to 25-nm-half-period features, which is consistent with our resolution test pattern images. The response curve extends to a cutoff at 19-nm half-period. This compares favorably with a prediction of 17 nm, based on an ideal zone plates with an outer zone width of 25 nm and a partially coherent illumination with σ equal to 0.45.

One should note that however, because of the nature of the partial coherence imaging, the normalized response only approximates the true response of XM-1, which is given by its transmission cross coefficient.

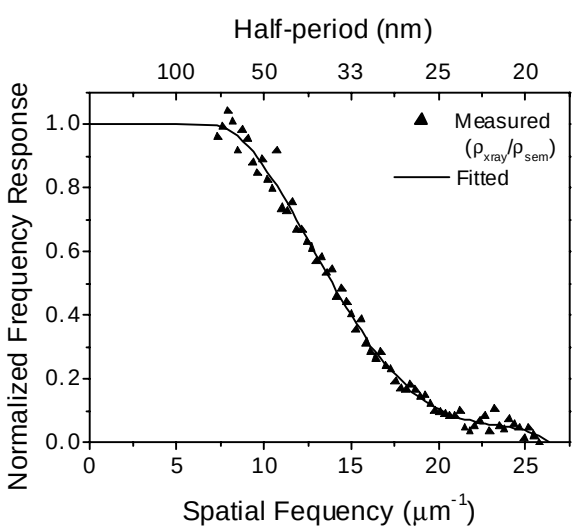

Figure 8. The normalized frequency response, obtained by dividing the power density of the soft x-ray image (ρ_{xray}) by that of the SEM image (ρ_{sem}), is plotted as a function of spatial frequency (bottom axis) and half period (top axis). 10% response is measured at a half period of 25 nm, which is consistent with our resolution measurements. The response cuts off around 19-nm half-period, which is slightly bigger than the theoretical cutoff of 17-nm half-period.

5. CONCLUSIONS

With the use of a bilayer-resist process, high-efficiency zone plates with an aspect ratio of 5:1 were fabricated successfully. These lenses improve diffraction efficiency, and thus greatly shorten the exposure time of our images. Along with a new beamline mirror, the MZPs enable the microscope to perform very-high-resolution imaging up to 2 keV energy range. Our next step is to extend our fabrication process to high-efficiency zone plates with finer zones.

ACKNOWLEDGEMENTS

This work was supported by the Director, Office of Science, Office of Basic Energy Sciences, of the U.S. Department of Energy, by DARPA, of the U.S. Department of Defense, and by the Air Force Office of Scientific Research.

REFERENCES

1. W. Meyer-Ilse, H. Medecki, L. Jochum, E. Anderson, D. Attwood, C. Magowan, R. Balhorn, M. Moronne, D. Rudolph, G. Schmahl, "New High-resolution Zone-plate Microscope at Beamline 6.1 of the ALS," *Synchrotron Radiation News*, **8**, pp. 22-23 (1995)
2. G. Denbeaux, E. Anderson, W. Chao, T. Eimüller, L. Johnson, M. Köhler, C. Larabell, M. Legros, P. Fischer, A. Pearson, G. Schütz, D. Yager and D. Attwood, "Soft X-ray microscopy to 25 nm with applications to biology and magnetic materials," *Nuclear Instruments and Methods in Physics Research Section Accelerators, Spectrometers, Detectors and Associated Equipment*, Volumes 467-468, Part 2, pp. 841-844 (2001)
3. E. H. Anderson, D. L. Olynick, B. Harteneck, E. Veklerov, G. Denbeaux, W. Chao, A. Lucero, L. Johnson, and D. Attwood Jr., "Nanofabrication and Diffractive Optics For High-Resolution X-Ray Applications," *J.Vac. Sci. Techn. B* **18**(6), 2970-2975 (2000)
4. W. Chao, E. H. Anderson, G. Denbeaux, B. Harteneck, M. Le Gros, A. L. Pearson, D. Olynick, D. Attwood, "High Resolution Soft X-ray Microscopy," *Soft X-Ray and EUV Imaging Systems*, Edited by W. M. Kaiser and R. H. Stulen, SPIE 4146, pp. 171-175 (2000)
5. G. Denbeaux, L.E. Johnson, and W. Meyer-Ilses, "Spectroscopy at the XM-1," *X-Ray Microscopy*, Edited by W. Meyer-Ilsee, T. Warwick and D. Attwood, AIP, New York, 1999, pp. 478-483.
6. G. Denbeaux, P. Fischer, G. Kusinski, M. Le Gros, A. Pearson, and D. Attwood, "A Full Field Transmission X-ray Microscope as a tool for High-Resolution Magnetic Imaging," *IEEE Trans. on Magnetics*, **37**(4), pp. 2764-2766 (2001)
7. B. L. Henke, E. M. Gullikson and J. C. Davis, "X-Ray Interactions: Photoabsorption, Scattering, Transmission, and Reflection at E = 50-30,000 eV, Z = 1-92," *Atomic Data and Nucl.Data Tables*, **54**, 181 pp. 191-342 (1993). Current updates are maintained by E. M. Gullikson at http://www-cxro.lbl.gov/optical_constants/
8. G. Schneider, D. Hambach, B. Niemann, B. Kaulich, J. Susini, N. Hoffmann, and W. Hasse, "In situ x-ray microscopic observation of the electromigration in passivated Cu interconnects," *Appl. Phys. Lett.*, **74**, pp. 1936-1938 (2001)
9. G. Schneider, G. Denbeaux, F. Salmassi, and P. Nachimuthu, to be published.